

# Feasibility of unzipping polymer polyphthalaldehyde for extreme ultraviolet lithography

Ashish Rathore<sup>a,b,\*</sup>, Ivan Pollentier<sup>b</sup>, Sunkuru S. Kumar<sup>b,c</sup>,  
Danilo De Simone<sup>b</sup> and Stefan De Gendt<sup>a,b</sup>

<sup>a</sup>KU Leuven, Department of Chemistry, Leuven, Belgium

<sup>b</sup>Imec, Leuven, Belgium

<sup>c</sup>National Tsing Hua University, Department of Materials Science and Engineering,  
Hsinchu, Taiwan

## Abstract

**Background:** Polyphthalaldehyde (PPA)-based systems can be interesting candidates for extreme ultraviolet (EUV) lithography as dry development resists with simple chemistry.

**Aim:** We present EUV-induced mechanistic and contrast curve studies for the end-capped PPA.

**Approach:** Fourier transform infrared (FTIR) spectroscopy and desorption studies were conducted to understand the EUV-induced mechanistic pathway. Although, contrast curve analysis was used to check its feasibility for EUV-patterning.

**Results:** First, FTIR and desorption studies confirmed that the EUV-radiation is capable to remove the end-capping group and induce unzipping (direct depolymerization) reaction in the PPA polymer chain. Second, contrast curve analysis showed a gradual decrease in the film thickness with respect to the EUV dose, which is due to the low EUV sensitivity of the PPA polymer. A post exposure bake step is important to improve the contrast curve, as it helps to depolymerize any residual polymer remaining after exposure. Further, even though the polymer sublimates when exposed to the EUV radiation, eliminating the need to apply a wet development step, crosslinking at high doses causes deposition of residual film onto the wafer surface. Therefore, a thin film (below 20 nm) and a wet development process might be important to get clean patterns.

**Conclusion:** This study confirms that the end-capped PPA, with a simple patterning mechanism, can be a useful system for the development of new dry development resists for EUV lithography.

© 2021 Society of Photo-Optical Instrumentation Engineers (SPIE) [DOI: [10.1117/1.JMM.20.3.034602](https://doi.org/10.1117/1.JMM.20.3.034602)]

**Keywords:** photoresist; extreme ultraviolet lithography; polyphthalaldehyde; dry development resists; unzipping; depolymerization mechanism.

Paper 21037 received Apr. 10, 2021; accepted for publication Jun. 25, 2021; published online Jul. 14, 2021.

## 1 Introduction

With the recent introduction of extreme ultraviolet lithography (EUVL) as the new high-volume manufacturing process, the onus is on exploring systems that can work well for sub-20-nm resolution patterning. Chemically amplified resists (CARs), which were the major workhorse system used in the conventional deep ultraviolet lithography (DUVL) process, show exacerbated performance when applied to the EUVL process. The reasons for this are as follows. First, with the change of source energy from DUV (~6 eV) to EUV light (~91.6 eV), the light-matter interactions in the photoresist change from excitation chemistry to radiation chemistry. And despite a considerable effort to understand these interactions in the previous studies,<sup>1-5</sup> the details

\*Address all correspondence to Ashish Rathore, [ashish.rathore@imec.be](mailto:ashish.rathore@imec.be)

are still not clear. Second, CARs use an acid-diffusion mechanism for patterning, which is difficult to control and causes problems such as high roughness and stochastic failures in the high-resolution patterns.<sup>6</sup> And third, CARs are multi-component systems containing a base polymer solution, in which several other moieties such as photoacid generator (PAG) and quencher are blended in, which complicates the patterning process.<sup>7</sup> Therefore, there is an urgent need to identify and develop new systems with simpler chemistry and patterning mechanism for the EUVL process.

In recent years, there have been several studies on organic and inorganic-based alternative platforms,<sup>8–16</sup> however, most of them are still in the research and development phase and further material investigations are needed. One interesting system that has been barely explored for photolithography application in the past is protected (end-capped) polyphthalaldehyde (PPA).<sup>17</sup> The end-capping on this material can be removed by applying high-temperature or high-energy radiation such as electron-beam or x-ray, triggering complete depolymerization (unzipping), and sublimation without redeposition.<sup>18,19</sup> The main advantages of this platform compared to others (CAR or metal-oxide resists) are that the mechanism of the solubility switch is non-complicated and the sublimation process eliminates the need to apply a developer solvent and simplifies the lithography process. Initial lithography studies on end-capped PPA systems showed promising results, however, with the popularity of CARs for the DUVL process, further studies on PPA-based photoresist were so far overlooked. With the advent of the EUVL process and the hunt for next-generation photoresist systems, PPA-based systems have become interesting again.

In this study, EUV-induced chemical changes are studied to understand its unzipping mechanism. Further, the feasibility of PPA polymer is evaluated for the EUVL process. This research could prove helpful in the development of such non-CAR photoresist concepts for high-resolution patterning in the future.

## 2 Experimental Methodology

### 2.1 Materials

Electronic grade capped PPA powder (99%) is obtained under its commercial name Phoenix-81 from Allresist GmbH, Germany. The chemical structure and reaction schemes (for polymerization and end-capping) are provided in Appendix Figs. 5 and 6, respectively. The powder is diluted in electronic grade casting solvent anisole (99.7%) obtained from Sigma Aldrich. Other reagent such as isopropanol (IPA, 99.7%) was also obtained from Sigma Aldrich.

### 2.2 Methodology

#### 2.2.1 Chemical characterization by FTIR spectroscopy

The EUV-induced chemical changes in the photoresist system are studied by Fourier transform infrared (FTIR) spectroscopy. A 300-mm Si wafer is spin coated with the photoresist material and different square regions ( $3 \times 3$  cm) are exposed with variable EUV-dose range. The exposed coupons are cut out and the residual film is analyzed with a Nicolet 6700 FTIR spectrometer.

#### 2.2.2 EUV-induced desorption studies

EUV-induced desorption is studied by the residual gas analyzer (RGA) setup installed in Imec's outgas tool.<sup>20,21</sup> Exposure to EUV-radiation causes chemical changes in the resist bulk and results in the desorption of certain volatile species, which are captured by RGA. The desorbing species are ionized by electron impact and analyzed by a quadruple mass spectrometer to obtain a fragmentation mass spectrum. The species are identified by comparing the spectrum with the NIST database.<sup>22</sup> The detailed setup and the description of the outgas tool can be found elsewhere.<sup>21</sup>

### 2.2.3 Contrast curve analysis

A contrast curve of the photoresist is analyzed on Imec's outgas tool<sup>20,21</sup> mounted with an EUV source to check the chemical contrast of the photoresist systems. The photoresist solution is coated on a 200-mm Si wafer and multiple points are exposed to a variable EUV-dose range in an open-frame experiment and the changes in the film thickness are checked with an ellipsometer. A wet development step is also applied to the wafer for cleaning the trenches and results are compared with the dry process.

## 3 Results and Discussion

### 3.1 Chemical Characterization by FTIR Spectroscopy

FTIR spectroscopy is used to check if the EUV radiation can induce unzipping in the end-capped PPA system and the result is shown in Fig. 1. The two interesting peaks that are used in this study are at wavenumber 1750 and 1000  $\text{cm}^{-1}$ , which represent C=O stretching (aldehyde carbonyl group of the depolymerized monomer) and C—O stretching (of original polymer), respectively. The area of the C=O peak shows an increase, whereas the area of the C—O peak shows a decrease with increasing EUV dose. This suggests the conversion of linear PPA polymer into its monomer and confirms the presence of an unzipping mechanism in the EUV-exposed end-capped PPA system. To get more details into the mechanism, the EUV-induced desorption experiment is carried out and the results are presented in the next section.

### 3.2 EUV-Induced Desorption

EUV-induced desorption studies are carried at a dose of 30  $\text{mJ}/\text{cm}^2$  to understand the unzipping mechanism of end-capped PPA, and the mass spectrum is shown in Fig. 2(a). The major peak at  $m/z$  134 is the volatile species called 1(3H)-isobenzofuranone ( $\text{C}_8\text{H}_6\text{O}_2^+$ ), and other peaks at  $m/z$  105 ( $\text{C}_6\text{H}_5\text{C}=\text{O}^+$ ), 77 ( $\text{C}_6\text{H}_5^+$ ), 63 ( $\text{C}_5\text{H}_3^+$ ), 51 ( $\text{C}_4\text{H}_3^+$ ), and 39 ( $\text{C}_3\text{H}_3^+$ ) are the subsequent fragments of this molecule.  $M/z$  118 is due to the loss of CO from the pyrone ring to form the Benzofuran ring ( $\text{C}_8\text{H}_6\text{O}^+$ ), another loss of CO results in the formation of  $\text{C}_7\text{H}_6^+$  ion at  $m/z$  90 and further H-loss forms  $\text{C}_7\text{H}_5^+$  ion at  $m/z$  89, as also described previously in the literature.<sup>23,24</sup>  $M/z$  44 and 29 correspond to the  $\text{CH}_3\text{CHO}$  and  $\text{CHO}$  peaks, respectively, and are byproducts of the end-capping group. The structures of major fragments are provided in Fig. 2(b). Based on the desorption studies, an EUV-induced unzipping pathway is proposed [Fig. 2(c.1)], in which the EUV-radiation induces a formation of a radical

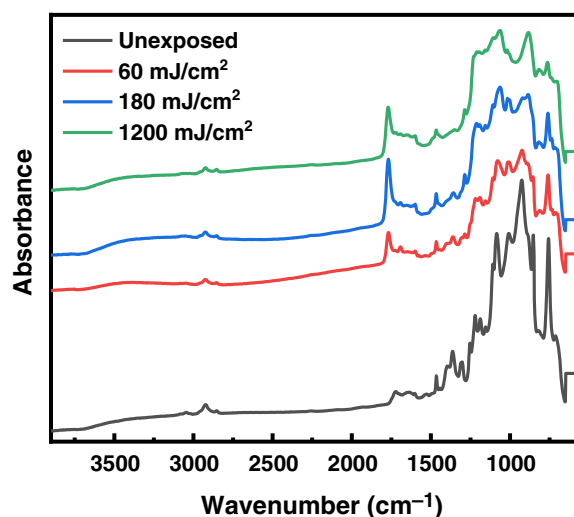
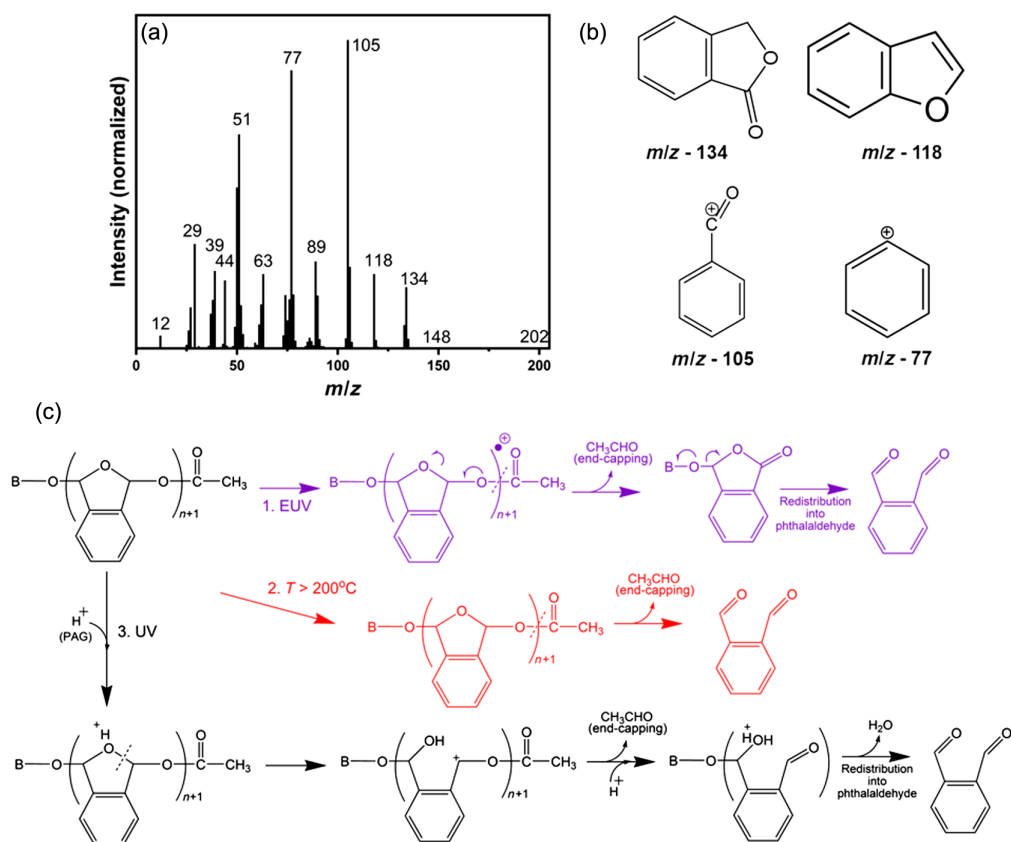


Fig. 1 FTIR analysis of end-capped PPA system.



**Fig. 2** (a) Fragmentation mass spectrum of end-capped PPA system exposed with an EUV dose of 30 mJ/cm<sup>2</sup>; (b) structures of major fragments with  $m/z$  134 (o-phthalaldehyde), 118 (benzofuran ring), 105 (C<sub>6</sub>H<sub>5</sub>C = O<sup>+</sup>), 77 (C<sub>6</sub>H<sub>5</sub><sup>+</sup>), and 44 (CH<sub>3</sub>CHO from end-capping); and (c) simplified (1) EUV-induced, (2) thermal-induced,<sup>25</sup> and (3) UV-induced unzipping pathway<sup>26</sup> (in the presence of PAG) of end-capped PPA.

cation, which causes removal of the end-capping functionality and forms a transient stable species of  $m/z$  134 (1(3H)-isobenzofuranone), as observed in the RGA experiments. This species can undergo further redistribution to form the monomer, phthalaldehyde. This pathway is similar to the thermal-induced unzipping mechanism of end-capped PPA when baked at a temperature of 200°C and above [Fig. 2(c.2)], as reported previously in the literature.<sup>25</sup> Adding PAG molecules in the PPA changes the unzipping mechanism significantly, as, upon exposure to UV-light, the generated acid molecules can protonate the acetal linkages and facilitate the unzipping mechanism [Fig. 2(c.3)], which improves the sensitivity of the material. The next step is to evaluate the capability of this system for the EUVL process by checking its contrast curve.

### 3.3 Contrast Curve Analysis

The chemical contrast of end-capped PPA is analyzed by exposing the 30-nm film to a variable EUV dose of 0 to 1800 mJ/cm<sup>2</sup> as shown in Fig. 3. No postexposure bake (PEB) and developer were applied for this process. The change in film thickness shows a linear decrease (with a slope of  $-0.132$  per mJ/cm<sup>2</sup>) with the EUV dose, which suggests a positive tone process. However, the chemical contrast is gradual (not very sharp) for EUV radiation. Also even after exposing the system at a high dose of 1800 mJ/cm<sup>2</sup>, the film is not completely removed from the wafer. This suggests that EUV exposure alone is incapable to depolymerize all the PPA chains. This is due to the low optical absorption of PPA film at EUV (13.6 nm) wavelength, which is calculated to be around 15% at 30-nm film thickness.<sup>27</sup> Therefore, the contrast and the residual film issue after

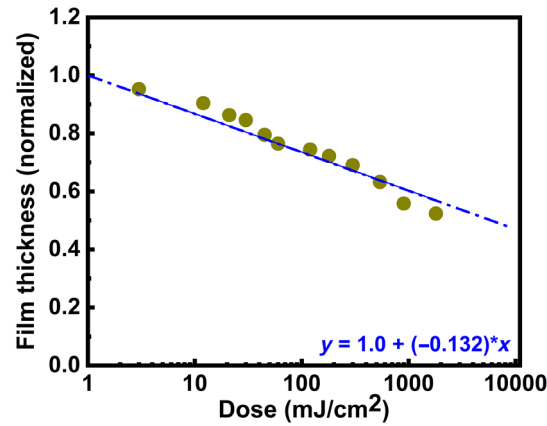


**Fig. 3** Contrast curve analysis of 30-nm-thick PPA film for a variable EUV dose.

exposure could be improved by adding a PEB and a wet development step, and the results are provided in the next section.

### 3.4 Effect of PEB and Wet Development Step on the Chemical Contrast

A PEB step with different temperatures is added after EUV exposure to try and improve the chemical contrast and sensitivity of the PPA system, as shown in Fig. 4(a). A PEB step of 90°C applied for 3 min does not show any improvement compared to the no PEB experiment, as observed by their slope values of  $-0.132$  and  $-0.130$  per  $\text{mJ}/\text{cm}^2$ , respectively. However, as the PEB is increased to 110°C (applied for 3 min), the contrast starts to improve as shown by the slope value of  $-0.164$  per  $\text{mJ}/\text{cm}^2$ . Further improvement can be achieved by applying the 110°C PEB step for a longer time, for example, 10 min, which gives a slope value of  $-0.191$  per  $\text{mJ}/\text{cm}^2$ . Even after applying a PEB of 110°C for 10 min, there is still a residual film remaining on the exposed part of the wafer. The saturation point and residual film ( $\sim 5$  nm) can be a sign that some of the monomers crosslink at a high EUV dose and temperature and can therefore not be sublimated from the wafer. This “tone-reversal” effect has also been seen in other polymers such as PMMA at high EUV doses.<sup>28</sup>

Finally, a thinner coating (of 18 nm) as well as a wet development step with anisole:IPA (1:3 v/v) developer with a 10-s IPA rinse, shows further improvements in chemical contrast and

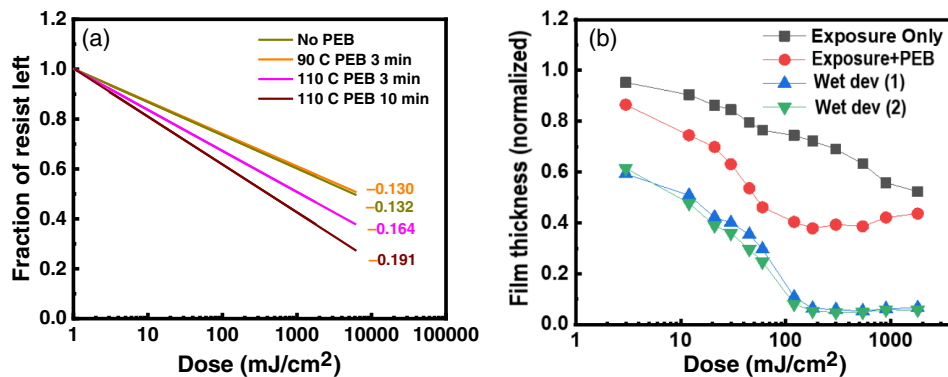


**Fig. 4** Effect of (a) PEB on chemical contrast (marked with their slope values) and (b) comparison with a wet development process with anisole:IPA (1:3 v/v) mixture on the end-capped PPA system. Wet development condition 1 refers to anisole:IPA (1:3) developer applied for 20-s plus a 10-s IPA rinse. Condition 2 refers to anisole:IPA (1:3) developer applied for 30-s plus a 10-s IPA rinse step.

removal of the residual film from the exposed regions [Fig. 4(b)]. Further, the 18-nm film of end-capped PPA still needs a high dose-to-clear ( $E_0$ ) value of over 100 mJ/cm<sup>2</sup>, due to its low EUV sensitivity. Therefore, additional groups or components need to be added to the end-capped PPA system to improve its contrast and sensitivity.

## 4 Conclusion

The PPA-based system can be an interesting prospect for the development of a dry development photoresist for the EUVL process in the future. In this work, the EUV-induced mechanism of end-capped PPA along with the contrast curve is analyzed to check its capability for the EUVL process. FTIR spectroscopy confirmed that the EUV radiation can remove the end-capping molecule and initiate the unzipping mechanism in the PPA polymer. EUV-induced desorption study showed the desorption of 1(3H)-isobenzofuranone and related volatile fragments, proving the complete depolymerization of PPA. Based on the desorption study, an EUV-induced mechanism of end-capped PPA is proposed, where the irradiation causes the formation of a radical cation on the O-center of the main chain and facilitate the removal of end-capping functionality, causing unzipping. This mechanism is similar to the thermal-induced unzipping of end-capped PPA but significantly different from the previously reported acid-induced mechanism upon UV exposure. The contrast curve of the end-capped PPA film (30 nm) in a dry development process showed a gradual decrease in the film thickness with increasing EUV dose. A PEB step of 110°C applied for 3 and 10 min showed significant improvements in the contrast values. However, the PEB step alone was insufficient to remove the film completely and a thin residual film remained on the exposed part of the wafer. Therefore, a thinner film (18 nm) was used, and a wet development step with anisole:IPA (1:3 v/v) developer was added to remove the residual film and further improve the contrast. The dose-to-clear ( $E_0$ ) value of 18 nm end-capped PPA film was determined to be >100 mJ/cm<sup>2</sup> from the contrast curve analysis, and further improvements are needed to enhance its EUV sensitivity.

## 5 Appendix

### 5.1 End-Capped Polyphthalaldehyde

Figure 5 presents the chemical structures of the PPA polymer, its monomer Phthalaldehyde, and the end-capped PPA.

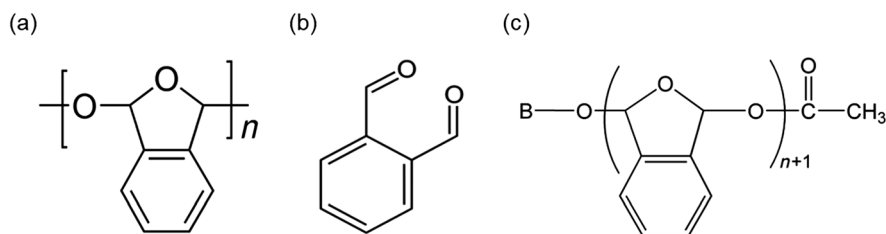


**Fig. 5** Chemical structure of (a) linear PPA polymer, (b) its monomer, 1(3H)-isobenzofuranone, and (c) the end-capped PPA.

### 5.2 Polymerization and End-Capping Scheme of PPA

Figure 6 presents the polymerization and end-capping step to synthesize end-capped PPA from its monomer.

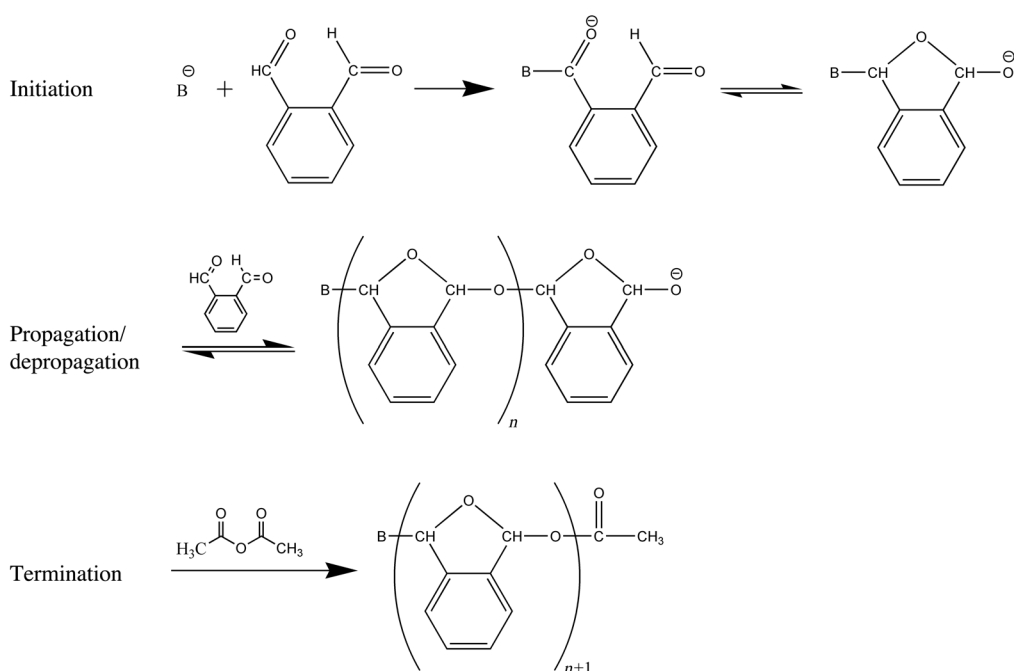


**Fig. 6** Reaction scheme of anionic polymerization of PPA and stabilization with the end-capping group.<sup>29</sup>

## Acknowledgments

This project had received funding from the European Union's Horizon 2020 Research and Innovation Program under the Marie Skłodowska-Curie Grant Agreement No. 722149 with the acronym "ELENA," which provides the PhD grant funding for A.R.

## References

1. A. Narasimhan et al., "Studying electron-PAG interactions using electron-induced fluorescence," *Proc. SPIE* **9779**, 97790F (2016).
2. A. Narasimhan et al., "Mechanisms of EUV exposure: electrons and holes," *Proc. SPIE* **10143**, 101430W (2017).
3. R. Gronheid et al., "Extreme-ultraviolet secondary electron blur at the 22-nm half pitch node," *J. Micro/Nanolithogr. MEMS MOEMS* **10**(3), 033004 (2011).
4. T. Kozawa et al., "Analysis of acid yield generated in chemically amplified electron beam resist," *J. Vac. Sci. Technol. B: Microelectron. Nanometer Struct. Process. Meas. Phenom.* **24**(6), 3055–3060 (2006).
5. H. Tsubaki et al., "EUV resist materials design for 15 nm half pitch and below," *J. Photopolym. Sci. Technol.* **26**(5), 649–657 (2013).
6. S. Tarutani et al., "Characterizing polymer bound PAG type EUV resist," *J. Photopolym. Sci. Technol.* **24**(2), 185–191 (2011).
7. L. Li et al., "Extreme ultraviolet resist materials for sub-7 nm patterning," *Chem. Soc. Rev.* **46**(16), 4855–4866 (2017).
8. M. Trikeriotis et al., "Development of an inorganic photoresist for DUV, EUV, and electron beam imaging," *Proc. SPIE* **7639**, 76390E (2010).
9. M. Trikeriotis et al., "A new inorganic EUV resist with high-etch resistance," *Proc. SPIE* **8322**, 83220U (2012).
10. M. Trikeriotis et al., "Nanoparticle photoresists from  $HfO_2$  and  $ZrO_2$  for EUV patterning," *J. Photopolym. Sci. Technol.* **25**(5), 583–586 (2012).
11. Y. Ekinici et al., "Evaluation of EUV resist performance with interference lithography towards 11 nm half-pitch and beyond," *Proc. SPIE* **8679**, 867910 (2013).

12. M. Toriumi et al., "Characterization of 'metal resist' for EUV lithography," *Proc. SPIE* **9779**, 97790G (2016).
13. S. Castellanos et al., "Ti, Zr, and Hf-based molecular hybrid materials as EUV photoresists," *Proc. SPIE* **10583**, 105830A (2018).
14. B. Cardineau et al., "Photolithographic properties of tin-oxo clusters using extreme ultraviolet light (13.5 nm)," *Microelectron. Eng.* **127**, 44–50 (2014).
15. N. Thakur et al., "Zinc-based metal oxoclusters: towards enhanced EUV absorptivity," *Proc. SPIE* **10957**, 109570D (2019).
16. C. Luo et al., "Review of recent advances in inorganic photoresists," *RSC Adv.* **10**(14), 8385–8395 (2020).
17. H. Ito et al., "Chemical amplification in the design of dry developing resist materials," *Polym. Eng. Sci.* **23**(18), 1012–1018 (1983).
18. K. Hatada et al., "Highly sensitive self developing electron-beam resist of aldehyde copolymer," *Polym. Bull.* **8**(9), 469–472 (1982).
19. C. G. Willson et al., "Chemical amplification in the design of polymers for resist applications," *Int. Union Pure Appl. Chem.* **28**, 448 (1982).
20. I. Pollentier et al., "Unraveling the role of secondary electrons upon their interaction with photoresist during EUV exposure," *Proc. SPIE* **10450**, 104500H (2017).
21. I. Pollentier et al., "Measurement and analysis of EUV photoresist related outgassing and contamination," *Proc. SPIE* **7271**, 727146 (2009).
22. "NIST Chemistry Webbook," <https://webbook.nist.gov/chemistry/>.
23. V. Lopez-Avila and G. Yefchak, "Mass spectral fragmentation studies of coumarin-type compounds using GC high-resolution MS," *Open Anal. Chem. J.* **5**(1) 27–36 (2011).
24. Q. N. Porter, *Mass Spectrometry of Heterocyclic Compounds*, 2nd ed., John Wiley & Sons, New York (1985).
25. M. Tsuda et al., "Chemically amplified resists. IV. Proton-catalyzed degradation mechanism of poly (phthalaldehyde)," *J. Photopolym. Sci. Technol.* **6**(4), 491–494 (1993).
26. K. M. Lee et al., "Phototriggered depolymerization of flexible poly (phthalaldehyde) substrates by integrated organic light-emitting diodes," *ACS Appl. Mater. Interfaces* **10**(33), 28062–28068 (2018).
27. B. L. Henke, E. M. Gullikson, and J. C. Davis, "X-ray interactions: photoabsorption, scattering, transmission, and reflection at  $E = 50\text{--}30,000$  eV,  $Z = 1\text{--}92$ ," *At. Data Nucl. Data Tables* **54**(2), 181–342 (1993).
28. A. Rathore et al., "Effect of molecular weight on the EUV-printability of main chain scission type polymers," *J. Mater. Chem. C* **8**(17), 5958–5966 (2020).
29. H. Ito and C. G. Willson, "Applications of photoinitiators to the design of resists for semiconductor manufacturing," *ACS Polym. Electron.* **242**, 11–23 (1984).

Biographies of the authors are not available.